



Effect of Nusselt Number Dependence on Reynolds Number in Solar Air Heaters of Varying Constructal Rib Geometries

Isaac F. Odesola¹, Ebenezer O. Ige^{1,2*} and Akeem B. Adebisi¹

¹Department of Mechanical Engineering, University of Ibadan, Ibadan, Nigeria.

²Department of Mechanical and Mechatronics Engineering, Afe Babalola University, Ado-Ekiti Nigeria.

Authors' contributions

This work was carried out in collaboration between all authors. Author IFO designed the study and wrote the protocol. Author EOI managed the analyses of the study and wrote the first draft of the manuscript. Author ABA managed the literature searches and supported in the analyses of the study. All authors read and approved the final manuscript.

Article Information

DOI: 10.9734/CJAST/2017/32359

Editor(s):

(1) Grzegorz Golanski, Institute of Materials Engineering, Czestochowa University of Technology, Poland.

Reviewers:

(1) Imdat Taymaz, Sakarya University, Turkey.

(2) A. Manivannan, Anna University, India.

(3) Obiekea Kenneth Nnamdi, Ahmadu Bello University, Nigeria.

Complete Peer review History: <http://www.sciencedomain.org/review-history/20140>

Original Research Article

Received 22nd February 2017

Accepted 8th May 2017

Published 20th July 2017

ABSTRACT

The most serious challenge in solar air heater is that the thermal performance is generally poor due to low heat transfer coefficient between the absorber plate and air flowing in the channel. Thermal performance in solar air heater is a critical issue because of usual low heat transfer coefficient. Hence, artificial roughness is being employed to enhance the rate of heat transfer in solar air heater. This study involved simulation of radiant air transport with geometric roughness such as square, rectangle and semi-circle rib. The operating parameter considered are; relative roughness height (e/D) values of 0.0283, 0.0566, 0.08500; relative roughness pitch (P/e) values ranged from 3.3 to 10 and the Reynolds number ranged from 100 to 2000 for standard laminar flow in a solar air heater. The absorber plate is heated with a uniform heat flux of 1000 W/m^2 for all the constructal ribs used in this study. The effect of geometric roughness investigated is based on both velocity and energy fields obtained via conservation principles of Navier-Stokes equations solved numerically on a finite

*Corresponding author: E-mail: ige.olubunmi@abuad.edu.ng, ige.bababunmi@gmail.com;

element based platform. Thereafter, the results obtained for Nusselt number (Nu) dependence on Reynolds number (Re) for various constructal rib geometries at selected roughness pitch investigated are here presented. For P/e at 3.33, Re ranged at 100 to 2000, Nu was observed to be 5.82 to 11.88; 11.32 to 17.98; 5.94 to 20.81; 0.85 to 9.33 for square, rectangle, semicircular and smooth ribs respectively. At P/e of 5.0 and investigated Re values, Nu was reported as 5.37 to 12.59; 9.72 to 16.20, 5.49 to 19.05, 0.85 to 9.33 for the respective constructal geometries. The Nu values obtained for P/e at 10.0 for the respective Re and geometric shapes 4.94 to 17.21, 14.71 to 33.61, 5.09 to 19.57, 0.86 to 9.33. The present study observed that Nusselt number considerably increased with roughness pitch for square and rectangular shaped rib geometries while it decreases slightly for semi-circle ribs but remains unchanged in smooth or rib-less ducts. Therefore, it can be concluded that rectangular and semi-circle shaped ribs offer a promising alternative in the design of micro solar-air heaters.

Keywords: Geometric roughness; thermal intensification; constructal design; ribs; duct flows.

NOMENCLATURE

Symbol	Physical quantity	Unit
V	velocity of air	ms^{-1}
T_o	Outlet temperature of duct length	K
T_i	inlet temperature of duct length	K
T_b	Bulk mean temperature	K
q	uniform heat flux	w/m^2
Q	heat transfer rate	W
ΔP	pressure drop in duct test section	Nm/s
K	thermal conductivity of air	$Wm^{-1}K^{-1}$
\dot{m}	mass flow rate of air	$kg s^{-1}$
C_p	Specific heat of the air	J kg K
Re	Reynolds number	Unitless
Pr	Prandtl number	Unitless
e	roughness height	mm
L	length of the duct	mm
D	depth of duct	mm
W	width of the duct	mm
H	height of the duct	mm
D_h	Hydraulic diameter	mm
Nu_r	Nusselt number for roughened duct	Unitless
Nu_s	Nusselt number for smooth duct	Unitless
Fr_r	Friction factor for roughened duct	Unitless
Fr_s	Friction factor for smooth duct	dimensionless
P	roughness pitch	mm
P/e	relative roughness pitch	Dimensionless
e/ D_h	relative roughness height	Dimensionless
Nu	Nusselt number	dimensionless
Fr	friction factor	dimensionless
h_r	convective heat transfer coefficient	$Wm^{-2}k^{-1}$
ρ	density of air	kgm^{-3}
ν	kinematic viscosity of air	$kgm^{-1}s^{-1}$
μ	dynamic viscosity	$N.s/m^2$
α	molecular diffusivity of heat	$kgm^{-1}s^{-1}$
Subscripts		
r	roughened	
s	smooth	
i	inlet	
o	Out	

1. INTRODUCTION

Solar air heater is one of the basic equipment through which solar energy is converted into thermal energy. The heat transfer characteristics of solar air heater have been widely studied. It has low heat transfer coefficient between absorber plate and the flowing air that results in higher heat losses to the environment which ultimately leads to low thermal efficiency of such thermal systems. In order to improve the heat transfer rate a fully turbulent flow in these systems has been achieved by Hikmet [1]. This increases the thermal heat transfer between the absorber-plate and the fluid, which clearly improves the thermal performances of the solar collector with obstacles arranged into the air channel duct. These obstacles allow a good distribution of the fluid flow as mentioned by N Moumami et al. [2].

There are different factors affecting the solar collector efficiency, e.g. collector geometry and dimensions, type of absorber surface, glass cover plate, air velocity etc. Increasing the absorber area or fluid flow heat-transfer area will increase the heat transfer to the flowing air on one hand and will increase the pressure drop in the collector, thus increasing the required power consumption to pump the air flow crossing the collector. The main application of solar air heaters are space heating, seasoning of timber, herbal medicine, curing of industrial products (textile and marine), crop drying, effectively used for curing/drying of concrete/clay building components and heating of buildings to maintain a comfortable environment especially during a winter season Tchinda, [3].

2. APPLICATION OF ARTIFICIAL ROUGHNESS

Whenever air flows over a heated surface, a very thin layer exists below the core turbulent region in which the flow remains predominantly laminar due to viscous effects called "laminar sub layer". Due to this viscous sub layer, the heat transfer rate from absorber surface to air is very low. Therefore the introduction of artificial roughness is to break that sub layer and creates local wall turbulence due to separation and reattachment of flow between two consecutive roughness elements. Thus instability created by various roughness elements significant enhances the heat transfer rates between the absorber surface & flowing fluid (air). Hence, artificial roughness in the form of ribs is commonly used in various

systems such as turbine blade cooling channels, heat exchangers, nuclear reactors and solar air heaters.

Many studies have been reported using experimental and theoretical approaches to improve the performance of solar heaters systems. Prasad and Saini [4] experimentally investigated the effects of the rib height and rib pitch on the heat transfer rate and friction factor in a solar air heater duct with transverse wire ribs on the absorber plate. Their results showed that the maximum enhancements in Nusselt number and friction factor were 2.38 and 4.25 times, respectively, compared with those observed in smooth ducts. Yadav and Bhagoria [5-7] numerically investigated the effects of transverse wire ribs, transverse square ribs, and transverse triangular ribs on the heat transfer and fluid flow characteristics in solar air heaters. The results showed that the average Nusselt number decreases with increasing the relative rib pitch, and it increases with increasing the relative rib height.

Singh et al. [8] performed a three-dimensional numerical investigation to study the effect of non-uniform cross-section transverse rib on the Nusselt number and friction factor of a solar air heater. Their results showed that the non-uniform cross-section saw-tooth rib results in higher Nusselt number than uniform cross-section ribs for Reynolds number above 7000. Promvong [9] experimentally investigated the friction and heat transfer characteristics in a rectangular channel fitted with multi V-shaped thin ribs. The results showed that, due to a better fluid mixing from the formation of secondary flows, the multi V-shaped ribs provide drastic increases in Nusselt number and friction factor over a smooth wall channel. Chaube et al. [10] conducted two dimensional CFD-based analysis of an artificially roughened solar air heater having ten different ribs shapes, namely, rectangular, square, chamfered, triangular, and so forth, provided on the absorber plate. CFD code, FLUENT 6.1 and SST k-w turbulence model were used to simulate turbulent airflow. The best performance was found with rectangular rib of size 3 x 5 mm, and CFD simulation results were found to be in good agreement with existing experimental results. Sharma and Thakur [11] conducted a CFD study to investigate the heat transfer and friction loss characteristics in a solar air heater having attachments of V-shaped ribs roughness at 60° relative to flow direction pointing downstream on underside of the absorber plate. Authors

observed, Nusselt number increases with increase in Reynolds number where friction factor decreases with increase in Reynolds number for all combinations of relative roughness height (e/D) and relative roughness pitch. Kumar and Saini [12] carried out CFD based analysis to fluid flow and heat transfer characteristics of a solar air heaters having roughened duct provided with artificial roughness in arc shaped geometry. The heat transfer and flow analysis of the chosen roughness element were carried out using 3-D models. Authors reported that Nusselt number has been found to increase with increase in Reynolds number where friction factor decreases with increase in Reynolds number for all combinations of relative roughness height (e/D) and relative arc angle ($\alpha/90$). Close [13] discussed solar air heaters for low and moderate temperature applications. It has been found that the main thermal resistance to the heat transfer is due to the formation of a laminar sub-layer on the heat transferring surface, which can be broken by providing artificial roughness on the heat-transferring surface. The artificial roughness has been used extensively for the enhancement of forced convective heat transfer, which further requires flow at the heat-transferring surface to be turbulent. However, the artificial roughness results in higher frictional losses leading to excessive power requirement for the fluid to flow through the duct, several works from Yadava group have investigated for square-sectioned [14], turbulence effect [15], artificial roughness effects [16,17], thermo-hydraulic effect solar air heaters using computational tools. The main purpose of this work is to study the effect of Nusselt Number Dependence on Reynolds Number in Solar Air heaters of varying Constructal Rib Geometries using computational fluid dynamics (CFD). The findings from this study are expected to benefit in design engineers in determination of optimized geometric shape and optimum thermal performance of solar-air dryers which could find usage in clean energy processing of agricultural produce.

2.1 Modeling and Numerical Simulation

Model of the solar air collector duct was designed according to the guidelines proposed in the ASHARE standard [18]. The entire solar collector was made of Aluminum and sectioned into three namely, Entrance length (L_1), Test length (L_2) and Exit length (L_3). The absorber plate's thickness was 0.5 mm which was placed on top of the test length of the channel and artificial roughness ribs with various ribs

geometries were mounted at the underside of the absorber plate in the channel running perpendicular to the flow direction is shown in Fig. 1. Fig. 2 represents simulation procedure in COMSOL multiphysics. The underneath and two sides of the collector were subjected to adiabatic condition. The geometrical and operating parameters employed in this CFD investigation are listed in the Table 2 and visualization of uniform mesh distribution for ribs are shown in the Figs. 3, 4 and 5.

Table 1. Thermo-physical properties of air and absorber plate for CFD analysis

Properties	Air	Aluminum
Density [kg/m^3]	1.225	2719
Specific heat [J/kgK]	1006.43	502.48
Thermal conductivity [$\text{Wm}^{-1}\text{K}^{-1}$]	0.0242	202.4
Viscosity [kg/m.s]	1.789×10^{-5}	

Table 2. Range of geometrical and operating parameters for CFD analysis

Geometry and operating parameter	Range
Entrance length of the Duct "L1" (mm)	240
Test length of the Duct "L2" (mm)	300
Exit length of the Duct "L3" (mm)	120
Width of the Duct "W" (mm)	150
Depth of the Duct "H" (mm)	20
Hydraulic Diameter of the Duct "D _h " (mm)	35.294
Duct aspect ratio "W/H"	7.5
Rib height "e" (mm)	1, 2 and 3
Rib pitch "P" (mm)	10, 20, 30 and 40
Reynolds number "Re"	100-2000
Prandth number "Pr"	0.7441
Relative roughness Pitch "P/e"	5, 10, 15, 20 and 2.5, 5, 7.5, 10 and 1.7, 3, 3.5, 6.7
Relative roughness height "e/D"	0.02833, 0.0567 and 0.08500
Uniform heat flux "I" (w/m^2)	1000

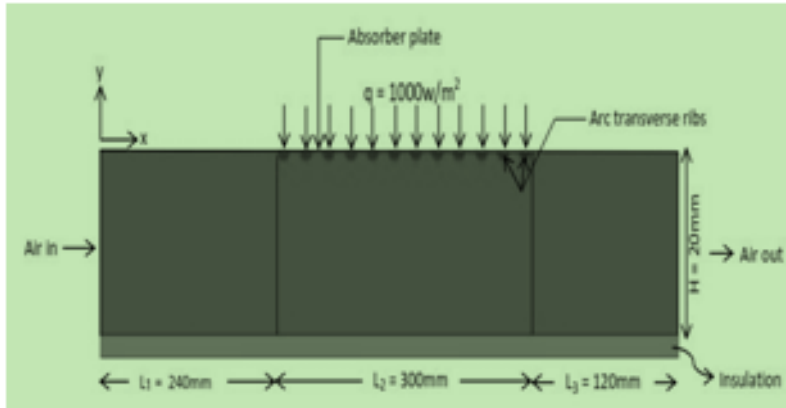


Fig. 1. Geometry of two dimensional computational domain for the solar air heater

2.2 Mesh Generation

Triangular mesh was generated around the Constructual geometries. The setting size for the meshes around the fluid element was selected and calibration was done to obtain the mesh statistics as: maximum element size 1.34, minimum element size 0.6, resolution of curvature 0.4, maximum element growth rate 1.2 was used for the simulation. Therefore, more cells were produced near the ribs which are very thin in nature when compared to the height of the flow field. All the meshes created in various shapes were user-controlled mesh and automatically generated. The analysis was carried out with 2D mesh in order to save the computer memory and time of computation.

2.3 Mathematical Modeling

The equation considered for this study was solved using finite element based COMSOL Multiphysics software packages for two-dimensional planes. The equations are continuity equation, Navier-stokes equation and energy equation. Post processing of results obtained was implemented using MATLAB. Assumptions were considered to simply the analysis. The assumptions are:

- (i) The solid material made of the entire domain is homogenous and isotropic except fluid (air).
- (ii) The working fluid is incompressible i.e. air for the operating range of solar air heaters.
- (iii) The flow is steady, fully developed, laminar and two dimensional.
- (iv) Thermal conductivity of the duct wall, absorber plate and the roughness elements does not change with temperature.

- (v) No-slip boundary condition was assigned to walls in contact with the fluid in the model.
- (vi) Heat losses and radiation heat transfer are negligible.

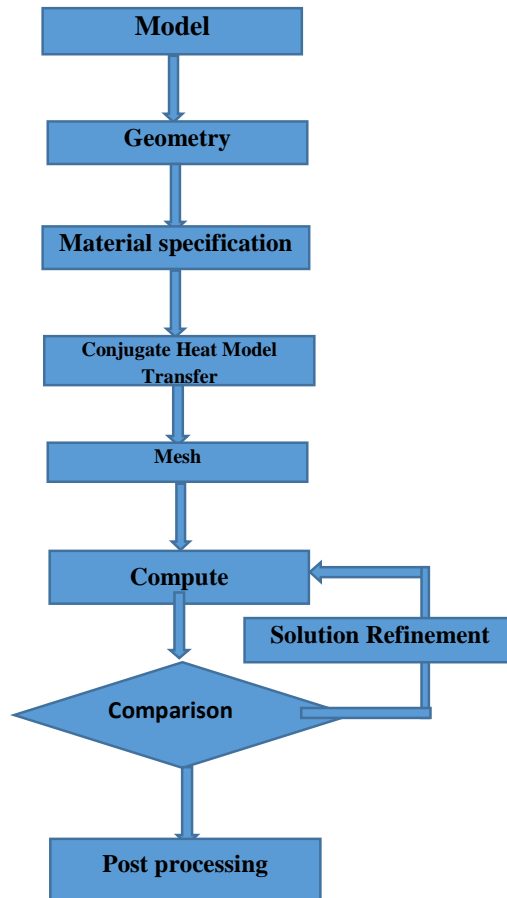


Fig. 2. Simulation procedure in COMSOL multiphysics

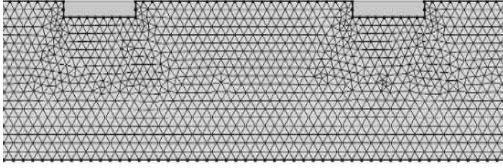


Fig. 3. Visualization of rectangle mesh distribution

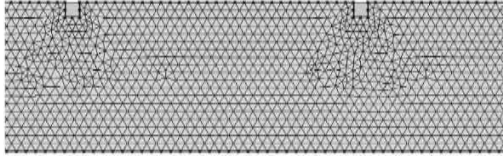


Fig. 4. Visualization of square mesh distribution

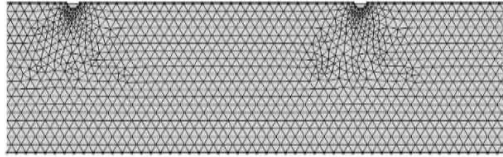


Fig. 5. Visualization of semi-circle mesh distribution

When the viscous dissipation is negligible, the continuity, momentum, and energy equations reduce for steady, incompressible, laminar flow of a fluid with constant properties over a flat plate to:

$$\text{Continuity equation } \frac{\partial u}{\partial x} + \frac{\partial v}{\partial y} = 0 \quad (1)$$

$$\text{Momentum equation } u \frac{\partial u}{\partial x} + v \frac{\partial u}{\partial y} = \frac{\mu}{\rho} \frac{\partial^2 u}{\partial y^2} \quad (2)$$

$$\text{Energy equation } u \frac{\partial T}{\partial x} + v \frac{\partial T}{\partial y} = \frac{\mu c_p}{k} \frac{\partial^2 T}{\partial y^2} \quad (3)$$

Where, $\alpha = \frac{v}{\rho r} = \frac{\mu c_p}{k}$ and the boundary condition are $u(x,0)=0, v(x,0)=0$ and

$$T(x,0)=T_s. \quad (4)$$

The hydraulic mean diameter of duct is determined as:

$$D_h = \frac{4(WH)}{2(W+H)} \quad (5)$$

The Reynolds number used defined as:

$$= \frac{UD_h}{\nu} \quad (6)$$

The convective heat transfer coefficient for the test section defined as

$$h_r = \frac{q}{T_w - T_b} \quad (7)$$

The average air temperature in the duct is defined as follows:

$$T_b = \frac{T_i - T_o}{2} \quad (8)$$

The dimensionless Nusselt number for artificially roughened solar air heater is obtained by

$$N_{ur} = \frac{h_r D_h}{k} \quad (9)$$

The dimensionless friction factor for the artificially roughened solar air heater is defined by

$$f_r = \frac{(\Delta p/L) D_i}{2\rho U^2} \quad (10)$$

3. RESULTS AND DISCUSSION

The graphs below shows the variation of Nusselt number on Reynolds number for various Constructal ribs obtained after simulation for various value of velocities, constant temperature and pressure.

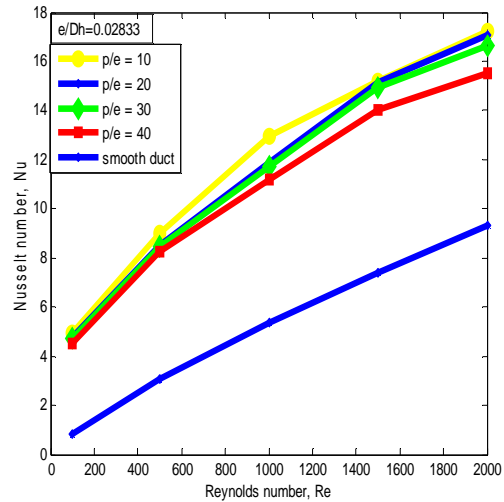


Fig. 6. Variation of Nusselt number on Reynolds number for square rib at roughness height (e=1)

For the Constructal geometric ribs investigated (square, rectangle and semi-circle) in this study, the numerical values of Nusselt number (rough) has been calculated from CFD analysis at

different Reynolds Numbers (100-2000), at fixed value of relative roughness height (0.0253) and varies the value of relative roughness pitch for Figs. 6, 7 and 8. It was observed that the value of Nusselt number obtained increases with the value of Reynolds number increases, due to interruption of the laminar sub-layer, which results into turbulence, separation and reattachment leading to higher heat transfer rate in the solar air heater. The value of Nusselt number is maximum for the rectangle transverse rib at 33.61 corresponding to the value of Reynolds number (2000).

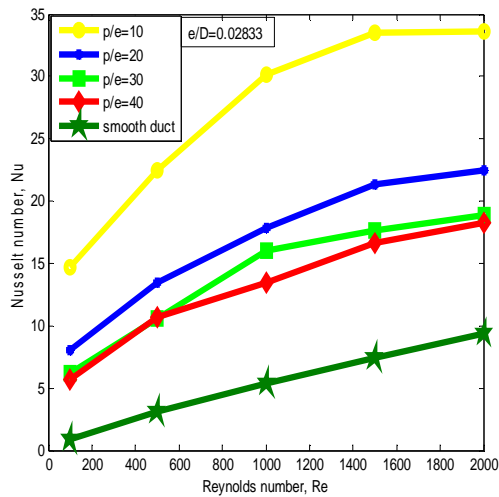


Fig. 7. Variation of Nusselt number on Reynolds number for rectangle at roughness height (e=1)

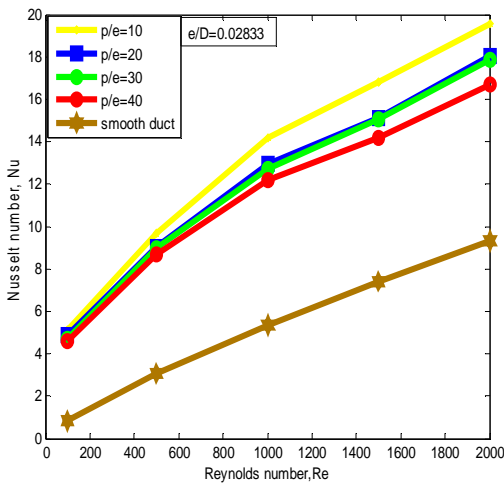


Fig. 8. Variation of Nusselt number on Reynolds number for semi-circle at roughness height (e=1)

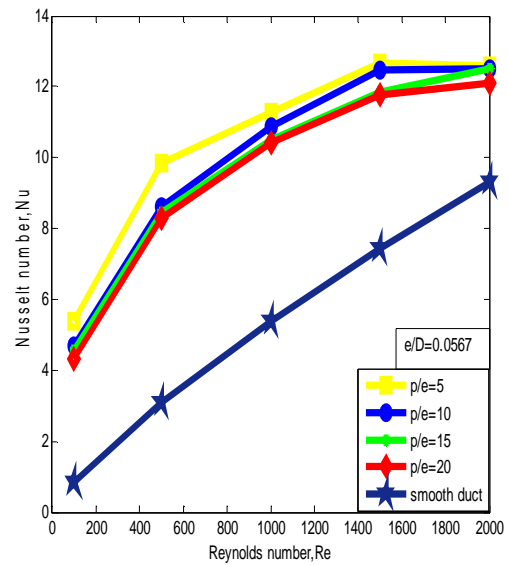


Fig. 9. Variation of Nusselt number on Reynolds number for square rib at roughness height (e=2)

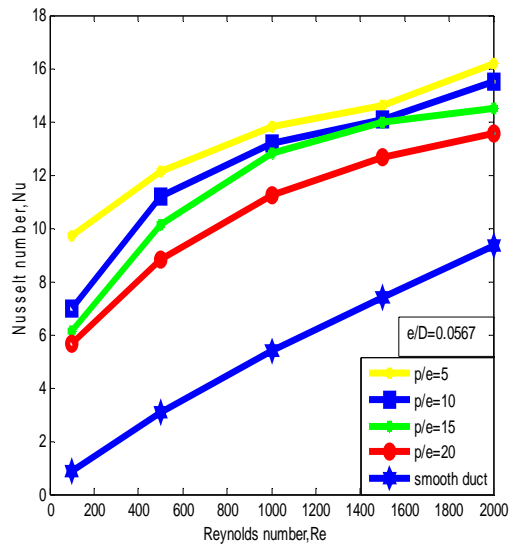


Fig. 10. Variation of Nusselt number on Reynolds number for rectangle rib at roughness height (e=2)

In case of Figs. 9, 10 and 11 increase in the Reynolds number leads to increase in Nusselt number in all geometry ribs. The Nusselt number is higher for semi-circle (19.06) at fixed relative roughness height value of 0.05667 for a Reynolds number value of 2000 for Fig. 11. It can be seen that the value of Nusselt number for ribs are higher when compared the value of

Nusselt number obtained for smooth duct. Therefore, heat transfer will be more in semi-circle transverse rib when compared to square transverse rib and rectangle transverse rib.

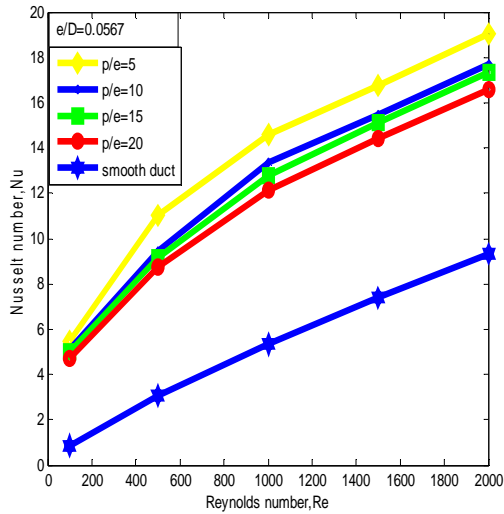


Fig. 11. Variation of Nusselt number on Reynolds number for semi-circle rib at roughness height (e=2)

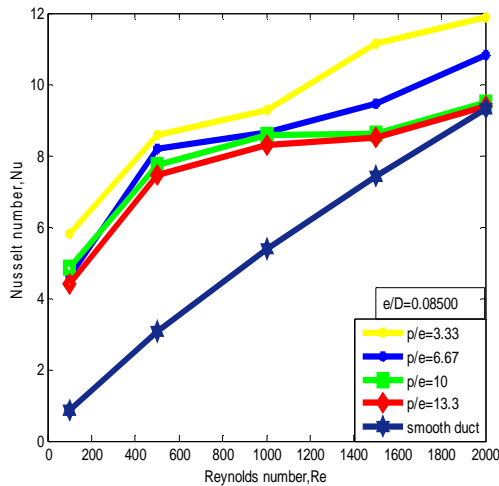


Fig. 12. Variation of Nusslet Number on Reynolds Number for Square roughness height (e=3)

number value of 2000 at fixed relative roughness height of 0.08500 when compared to Figs. 12 and 13.

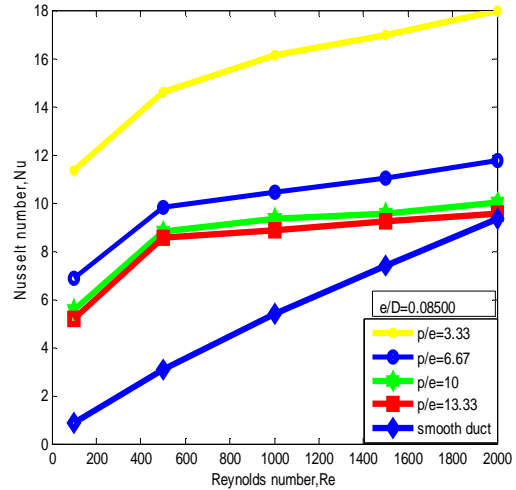


Fig. 13. Variation of Nusselt number on Reynolds number for rectangle at roughness height (e=3)

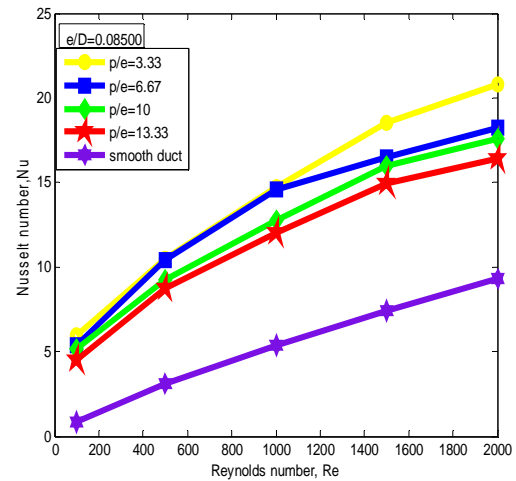


Fig 14. Variation of Nusselt number on Reynolds number for semi-circle at roughness height (e=3)

Figs. 12, 13 and 14 also show variation of Nusselt number with Reynolds number. It was observed that for all transverse ribs the Nusselt number increases with an increase in Reynolds number for roughened ribs as well as smooth duct considered. Fig. 14 has the highest Nusselt number of 20.81 corresponding to Reynolds

3.1 Validation of Results

The present CFD Numerical simulation result of the artificially roughened solar air heater with sectioned transverse rib roughness has been validated with results of authors mentioned above in Table 3. It can be seen that the range of Reynolds number of present study considered are extremely far while the relative roughness height and relative roughness pitch. Therefore,

the trends of the result are similar, since they all show appreciable heat transfer enhancement. Yadav and Bourgnia [19] concluded that Nusselt number values decrease with increase in the relative roughness pitch (P/e) for fixed relative roughness height (e/D). Also in the present study the value of Nusselt number decrease with increase in the relative roughness pitch (P/e) for fixed relative roughness height (e/D). This is due to the fact that with the increase in relative roughness pitch, number of attachment points over the absorber plate reduces. The maximum value of Nusselt number for this study is obtained at lower relative roughness pitch likewise the maximum value of Nusselt number was obtained at lower relative roughness pitch for Yadav & Bourgnia [20]. Also, Soi et al. [21] reported that relative roughness height (e/D) was kept fixed while relative roughness pitch was varied for a given type of artificial roughness, Nusselt number increase with an increase in Reynolds number for smooth as well as roughened plate which is in agreement with the present study.

Table 3. Comparison of present and previous study for CFD obtained

Parameters	Present study	Yadav and Bourgnia (2013)	Aman Soi (2010)
e/d	0.028	0.03	0.029
Re	100-2000	3000-18000	4000-16000
P/e	10	10	8.3
Nu	4-35	25-130	10-70

4. CONCLUSIONS

A 2D heat transfer in minichannels with geometric varieties of Constructal shapes has been investigated. Numerical analysis of different Constructal geometry parameters of artificial roughness on the absorber plate were performed for different configurations of rib roughness and values of Reynolds number (100 - 2000). In view of present CFD predictions the following conclusions are drawn:

- (1) It was found that for various construct rib geometry the dependence of Nusselt number increases with the increases in Reynolds number for various values of relative roughness pitch (p/e) and at constant relative roughness height (e/D_h).
- (2) The present study observed that Nusselt number considerably increased with

roughness pitch for square and rectangular shaped rib geometries while it decreases slightly for semi-circle ribs but remains unchanged in smooth or ribless ducts. Therefore, the conclusion can be made that rectangular and semi-circle shaped ribs offer a promising design application in construction of micro solar-air heaters.

- (3) The findings showed that geometric shape optimization could be insisted during design process for optimum utilization of thermal energy which could directly impact on the performance of the entire system set-up for solar air dryers.

COMPETING INTERESTS

Authors have declared that no competing interests exist.

REFERENCES

1. Esen Hikmet. Experimental energy and exergy analysis of a double-flow solar air heater having different obstacles on absorber plates. *Building and Environment*. 2008;43:1046-1054.
2. Moumni N, Youcef-Ali S, Moumni A, Desmons JY. Energy analysis of a solar air collector with rows of fins. *Renewable Energy*. 2004;29:2053–2064.
3. Tchinda R. A review of the mathematical models for predicting solar air heaters systems. *Renewable and Sustainable Energy Reviews*. 2009;13:1734–59.
4. Prasad BN, Saini JS. Effect of artificial roughness on heat transfer and friction factor in a solar air heater. *Sol Energy*. 1988;41:555-60.
5. Yadav AS, Bhagoria JL. A CFD (computational fluid dynamics) based heat transfer and fluid flow analysis of a solar air heater provided with circular transverse wire rib roughness on the absorber plate. *Energy*. 2013;55:1127-42.
6. Yadav AS, Bhagoria JL. A numerical investigation of square sectioned transverse rib roughened solar air heater. *Int J Therm Sci*. 2014;79:111-31.
7. Yadav AS, Bhagoria JL. A CFD based thermo-hydraulic performance analysis of an artificially roughened solar air heater having equilateral triangular sectioned rib roughness on the absorber plate. *Int J Heat Mass Transf*. 2014;70:1016-39.
8. Singh S, Singh B, Hans VS, Gill RS. CFD (computational fluid dynamics)

- investigation on Nusselt number and friction factor of solar air heater duct roughened with non-uniform cross-section transverse rib. *Energy*. 2015;84:509-17.
9. Promvong P. Heat transfer and pressure drop in a channel with multiple 60 V-baffles. *Int Commun Heat Mass Transf*. 2010;37:835-40.
 10. Chaube A, Sahoo PK, Solanki SC. Analysis of heat transfer augmentation and flow characteristics due to rib roughness over absorber plate of a solar air heater. *Renewable Energy*. 2006;31(3):317-331.
 11. Sharma AK, Thakur NS. CFD based fluid flow and heat transfer analysis of a V-shaped roughened surface solar air heater. *International Journal of Engineering Science and Technology*. 2012;4(5):2115-2121.
 12. Kumar S, Saini RP. CFD based performance analysis of a solar air heater duct provided with artificial roughness. *Renewable Energy*. 2009;34(5):1285-1291.
 13. Close DJ. Solar air heaters for low and moderate temperature application. *Solar Energy*. 1963;7:117-124.
 14. Yadav, Bourgnia. A CFD analysis of a solar air heater having triangular rib roughness on absorber plate. *Renewable Energy*. 2013;5(2):964-971.
 15. Anil Singh Yadav, Bhagoria JL. A numerical investigation of square sectioned transverse rib roughened solar air heater. *International Journal of Thermal Sciences*. 2014;79:111-131.
 16. Anil Singh Yadav, Bhagoria JL. A numerical investigation of turbulent flows through an artificially roughened solar air heater. *Numerical Heat Transfer, Part A: Applications*. 2014;65(7):679-698.
 17. ASHRAE Standard. Method of testing to determine the thermal performance of solar collectors. American Society of Heating, Refrigeration and Air Conditioning Engineers, Atlanta, GA30329; 2003.
 18. Anil Singh Yadav, Bhagoria JL. Heat transfer and fluid flow analysis of an artificially roughened solar air heater: A CFD based investigation. *Frontiers in Energy*. 2014;8(2):201-211.
 19. Anil Singh Yadav, Bhagoria JL. A CFD based thermo-hydraulic performance analysis of an artificially roughened solar air heater having equilateral triangular sectioned rib roughness on the absorber plate. *International Journal of Heat and Mass Transfer*. 2014;70:1016-1039.
 20. Anil Singh Yadav, Bhagoria JL. Numerical investigation of flow through an artificially roughened solar air heater. *International Journal of Ambient Energy*. 2015;36(2): 87-100.
 21. Amon Soi, Ranjit S, Bhushan B. Effect of roughness element pitch on heat transfer and friction characteristics of artificial roughened solar air heater duct. *Energy*. 2010;1:339-346.

© 2017 Odesola et al.; This is an Open Access article distributed under the terms of the Creative Commons Attribution License (<http://creativecommons.org/licenses/by/4.0>), which permits unrestricted use, distribution, and reproduction in any medium, provided the original work is properly cited.

Peer-review history:

The peer review history for this paper can be accessed here:
<http://sciencedomain.org/review-history/20140>